A-3.2.1 Studies on Atmospheric Trace Gas Measurements Using a Satellite-Borne Retroreflector (Final Report)

Contact Person Nobuo Sugimoto

Head, Upper-Atmospheric Environment Section
National Institute for Environmental Studies
Environment Agency
Onogawa, Tsukuba, Ibaraki 305, Japan
Phone +81-298-50-2459, Fax +81-298-51-4732
E-mail nsugimot@nies.go.jp

Total Budget for FY1995 - FY1997 74,089,000 Yen (FY1997; 20,642,000 Yen)

Abstract

Earth-satellite-earth laser long-path absorption method for measuring atmospheric trace species was demonstrated with the Retroreflector in Space (RIS) on the ADEOS, which was launched on August 16, 1996 by NASDA. In the initial experiments, optical characteristics of the RIS was evaluated and confirmed that It was working properly in orbit. The first atmospheric spectrum was measured with two TEA CO_2 lasers based on the method using the Doppler shift caused by the satellite movement. Column contents of ozone was derived from the spectrum. It was validated by the simultaneous measurement with a laser heterodyne spectrometer. The operation of the ADEOS was discontinued, unfortunately, on June 30, 1997 due to the malfunction with the solar panel. To evaluate the measurement method and measurement system, measurement error was analyzed using the data taken with the RIS. It was found that the noise due to slight difference in the laser beam pattern of the two lasers were the cause of the error. Based on the analysis, the transmitter system and the satellite tracking system were improved. Characteristists of errors were also studied by comparing with the errors in the measurements with a corner-cube retroreflector installed on a tower 4 km away from the ground station. Because of the discontinuance of the ADEOS operation, we were not able to obtain sufficient data for atmospheric studies. However, we were able to demonstrate the measurement techiniques for the first time, and we obtained useful data for the development of the next generation measurement system based on the earth-to-satellite laser long-path absorption method.

Key Words atmospheric trace gas, laser long-path absorption method, satellite retroreflector, RIS, ADEOS

1. Introduction

The laser long-path absorption method between the ground and a satellite is one of the most sensitive remote sensing techniques for measuring concentration of atmospheric trace species. The idea of the measurement using a satellite retroreflector was described in the paper by Hinkley in 1976 (Hinkley 1976), but experiment on this technique had not been implemented. The first experiment on Earth-satellite-Satellite laser long-path absorption technique was carried out with the RIS on the ADEOS.

The RIS was a 0.5-m diameter single-element hollow cube-corner retroreflector newly designed for the experiment. The RIS had a unique design using a spherical mirror to optimize the reflected beam pattern. The ground laser transmitter/receiver system used two single-longitudinal-mode

pulsed transverse, electric, atmospheric (TEA) CO_2 lasers. We measured spectrum of atmospheric ozone using the RIS by the Doppler shift method which utilized the Doppler shift of the return beam cause by the satellite movement. Figure 1 shows the concept of the RIS experiment.

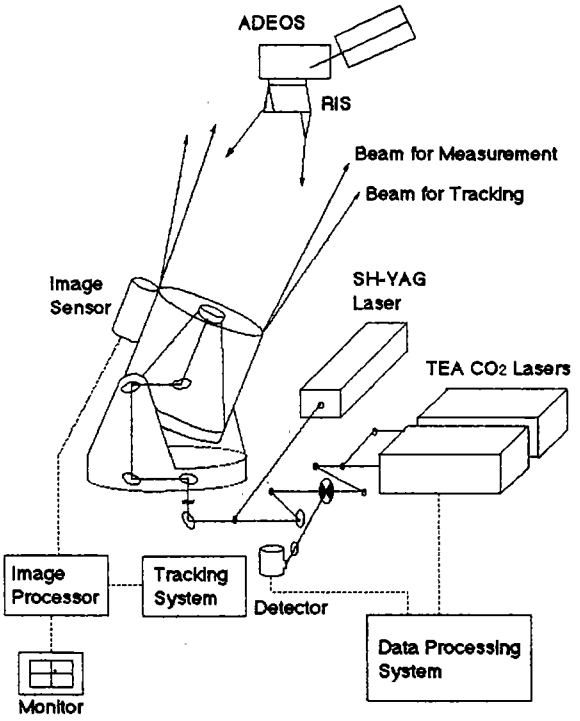

Fig. 1 Concept of the RIS experiment.

2. RIS on the ADEOS and the Ground System

The RIS is a hollow cube-corner retroreflector having a spherical mirror to control the pattern of the reflected beam. We determined the surface parameters of the RIS with a computer simulation so that sufficient received power is obtained in a wide angular range. Figure 2 shows the structure of the RIS. The mirror panels were made of quartz with light weighted structure. The surface was finished with a silver-based optical coating. The housing is made of aluminum. The RIS was installed on the ADEOS so that the optical axis is directed to the ground with an angle of 30 degree toward the direction of movement from nadir. The RIS can be used from a ground station when the RIS passes over one of the ground tracks within several hundred kilometers of the ground station and when the elevation angle is within the range from 30 degree to 90 degree.

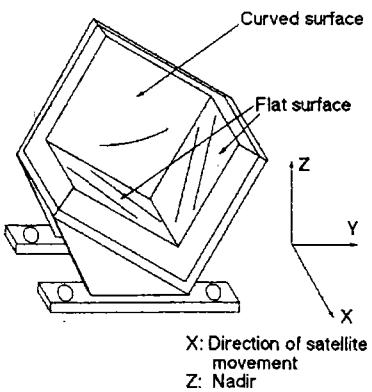

Fig. 2 Structure of the RIS.

The ground system consists of optical satellite tracking system and lasers for the spectroscopic measurement. Figure 3 illustrates the ground system.. We used the tracking telescope with a 1.5-m diameter at the Communications Research Laboratory in Koganei, Tokyo. A second-harmonics Nd:YAG laser performed active tracking by using the reflection image of the RIS, and was used for laser ranging to the ADEOS. The active tracking was performed concurrently with the programmed tracking to correct bias in programmed tracking. Two single-longitudinal-mode TEA CO_2 lasers were employed in the spectroscopic measurement (Nordstrom et al. 1993, 1994, Ozawa et al. 1997b). One of the lasers was used to measure the absorption of the target molecule, and the other to measure the reference signals to correct for atmospheric effects and the angular dependence of the RIS reflection.

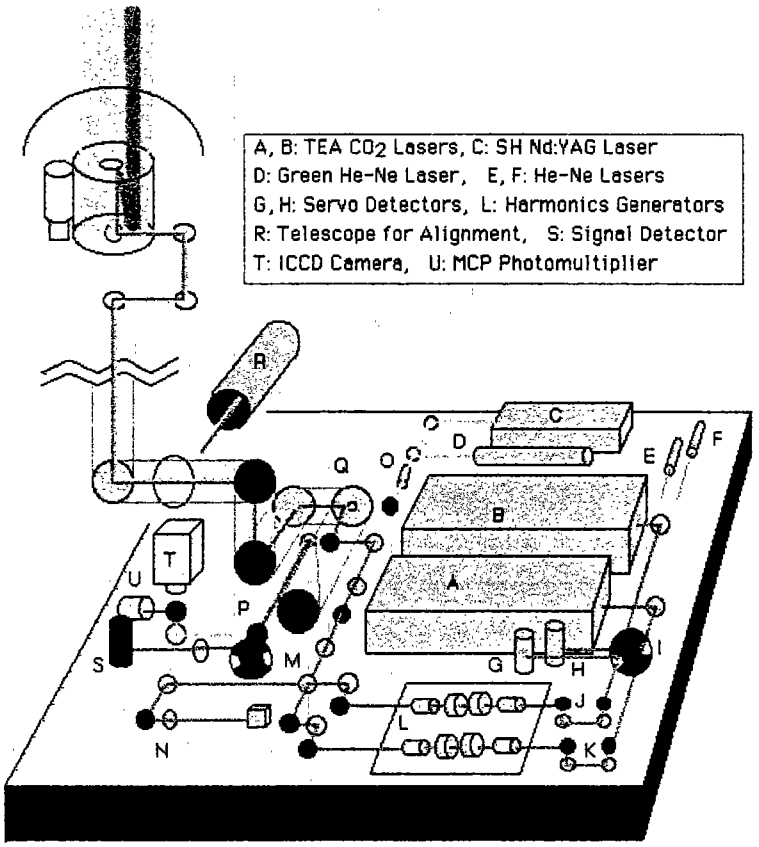

Fig. 3 Laser transmitter-receiver system for the RIS experiment.

We used the Doppler shift of reflected beam caused by the satellite's movement in the RIS experiment (Sugimoto et al. 1991, 1995b). Since the magnitude of the Doppler shift depends on the elevation angle to the ADEOS, the absorption spectra of the atmosphere can be measured using the change in the wavelength of the return beam. The Doppler shift can be expressed by

$$\Delta f = (2vf_0/c) \cos \theta, \qquad (1)$$

where v is velocity of satellite, f_0 is frequency of the laser, and θ is elevation angle to the satellite.

Since the speed of the ADEOS is 7 km/s, the spectral range covered by the Doppler shift is 0-1.3 GHz (0-0.04 cm^{-1}) at 10 μm.

The beams from the two lasers were collimated and combined with a half mirror. The combined beam was directed to the Coude path of the 1.5 m telescope and transmitted to the RIS. The repetition rate of the TEA lasers was 50 Hz, and time interval between pulses from two lasers was 200 μs. The transmitted pulse energy was approximately 50 mJ at 10 μm. The reflected signal from the RIS was collected with the same telescope and focused on a HgCdTe detector cooled at 77 K. A portion of the transmitted beam was picked off and directed to a room temperature HdCdTe detector to monitor the power. The wave forms of transmitted and received laser pulses were recorded at every shot with a high-speed transient digitizer. Time gate for recording the received pulse was predicted using the orbital parameters for the ADEOS satellite.

3. Optical Characteristics of the RIS in Orbit

Active tracking of the RIS was established using the image taken with the intensified charge coupled device (ICCD) camera in the Coude system of the 1.5-m diameter telescope. Accuracy better than 30 μrad was obtained by the active method both in the daytime and nighttime.

We measured the efficiency of the reflection from the RIS at 532 nm by comparing the image of the RIS lit by a second harmonics Nd:YAG laser with the images of stars. The efficiency, η (m^{-2}), is defined so that the received power is calculated by the following equation:

$$P = (16/\pi^2)\,(P_0/\theta_t^2)\,T^2\,\eta_{RIS}\,A_r\,\eta_{sys}\,\eta, \qquad (2)$$

where P_0, θ_t, T, η_{RIS} A_r, and η_{sys} represent transmitted power, divergence of the transmitted beam, transmittance of the atmosphere, reflectance of the RIS, aperture of receiver, and efficiency of the receiver system, respectively.

In the experiment, the beam from the Nd:YAG laser at 532 nm was diverged in the Coude path and transmitted from the 1.5-m primary mirror with a beam divergence of 0.5 mrad. Transmitted laser energy was 30 mJ/pulse. The reflection from the RIS was observed with the ICCD camera on the guiding telescope with a diameter of 20 cm. The intensity of the return was measured from the recorded image. We first measured images of stars with different stellar magnitudes, and confirmed the reproducibility of the intensity measurement. We also considered the difference between the continuous and pulsed light source. Since the Nd:YAG laser pulses with a repetition rate of 10 Hz, and the ICCD camera has an integration time of 1/30 sec, we needed to multiply the intensity of the laser reflection recorded in a frame by a factor of 1/3 to avoid overestimate the intensity. The return from the RIS measured with the ICCD camera was comparable to stellar magnitude of 2 to 3 depending on the elevation angle. We obtained the efficiency of the reflection from the RIS using Eq.(2). We assumed that T = 0.7 and η_{RIS} = 0.8. We calibrated the efficiency of the receiver system by the intensities of stars.

The measured efficiencies of the reflection from RIS for different paths are shown in Fig. 4(a) for nighttime paths and in Fig. 4(b) for daytime paths (Ozawa et al. 1997a). The maximum elevation angle for the path is higher in the upper path in each figures. The horizontal axis of Fig. 4 indicates the time that corresponds to the location of the ADEOS along the path. The elevation angle to the ADEOS reached maximum at the end of the measurement. The theoretical efficiencies for the same paths which were calculated based on the wave front of the RIS PFM are shown in Fig. 5(a) and (b) (Sugimoto et al. 1996). The measured efficiency was affected by atmospheric conditions and

tracking errors. There were occasional delay in the initial capture of the RIS, but the maximum efficiency for each path agreed well with the theory. We concluded from the comparison that the RIS was working very well in orbit.

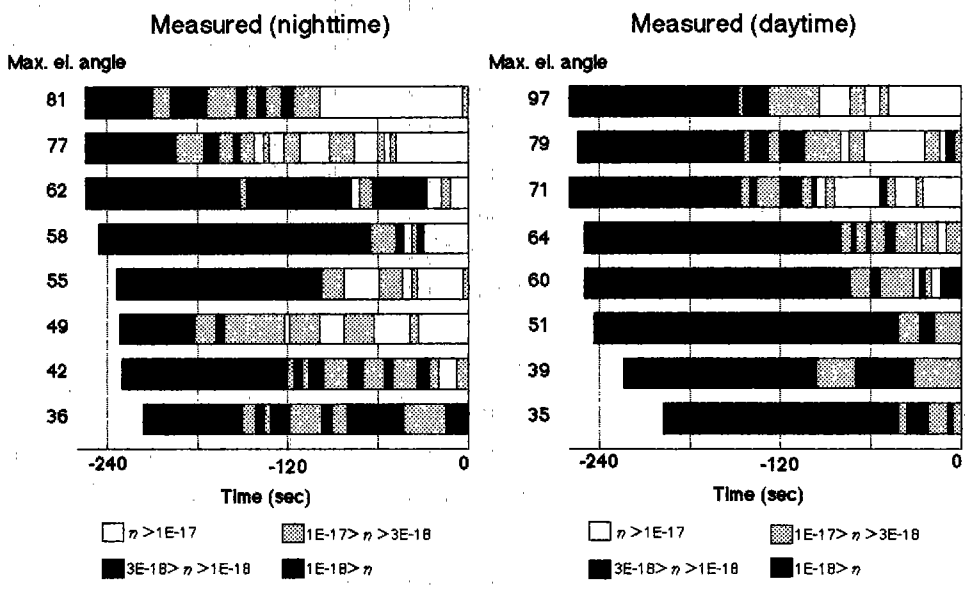

Fig. 4 Measured efficiency of reflection from RIS for different paths. (a) nighttime, (b) daytime.

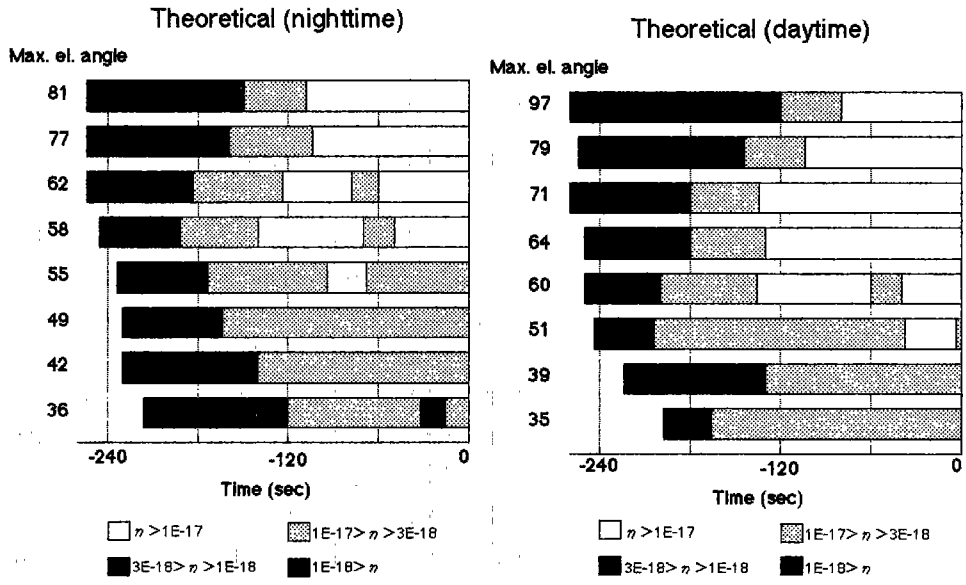

Fig. 5 Theoretical efficiency for the same paths as in Fig 4 calculated based on the wave front of the RIS PFM.. (a) nighttime, (b) daytime.

We evaluated the intensity of the infrared reflection from the RIS by comparing the return signal with that from a 3-cm hollow retroreflector installed on a tower located 4.2 km from the ground station. Figure 6 shows an example of wave forms of a pair of transmitted and received CO_2 laser pulses measured with the RIS. The recorded signal intensity from the RIS was comparable to that from the tower retroreflector when an optical attenuator of 10^{-5} was used with a 100 times smaller detector gain. Transmitted beam divergence for the RIS and tower reflector was

9.0 x 10^{-5} rad and 2.5 x 10^{-5} rad, and we assumed that the atmospheric transmittance was 0.9 for the RIS and 0.97 for the tower. The efficiency, h, for the tower retroreflector is 2.2 x 10^{-11} m^{-2}. Using these parameters, the efficiency for the RIS was estimated to be 3.3 x 10^{-17}. It agreed very well with the designed value 4 x 10^{-17} (Ozawa et al. 1997b).

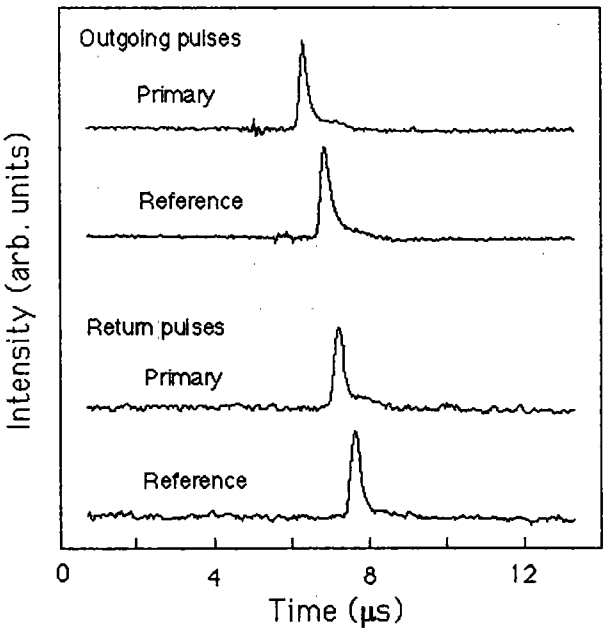

Fig. 6 Example of the recorded waveforms of a pair of transmitted and received CO_2 laser pulses at 10 μm.

4. Spectroscopic Experiment and Error Analysis

We carried out the experiments on the spectroscopic measurement using the TEA CO_2 lasers. Figure 6 shows a measured spectrum data with the RIS. The two TEA CO_2 lasers were tuned to the 10R(24) line of $^{13}CO_2$ and the 9P(24) line of $^{12}CO_2$, respectively. The vertical axis indicates the logarithm of the ratio of the signal intensity for the primary laser to that for the reference laser. The horizontal axis indicates shot number. The wavelength of the return light changes with the shot number due to the change in the Doppler shift. Laser pulses from the two lasers were with a repetition rate of 50 Hz, and 10,000 pulse pairs were recorded in a measurement.

Figure 8 shows simulated signals for the RIS measurement which was calculated based on the theoretical spectrum and the calculated efficiency of reflection for the RIS. The dip seen in the measured spectrum is due to the absorption of ozone that the 9P(24) line of $^{12}CO_2$ received. Because both the path length and the wavelength change in the measurement, the shape of the absorption is not symmetrical.

We derived column contents of ozone from the measured spectrum by fitting the theory with the least-squares method. The effect of the continuum absorption and the difference in optical efficiency for the system at the two wavelengths were determined at the same time in the least-squares fitting. The US Standard Atmosphere was used for the distribution of atmospheric CO_2. We obtained the column contents of ozone of 8.6 x 10^{18} cm^{-2}. To validate the measurement with

the RIS, we conducted a simultaneous measurement with a laser heterodyne spectrometer in cooperation with Tohoku University (Fukunishi et al 1990). Column contents obtained with the heterodyne spectrometer was 8.3 x 10^{18} cm^{-2} and agreed well with the RIS measurement.

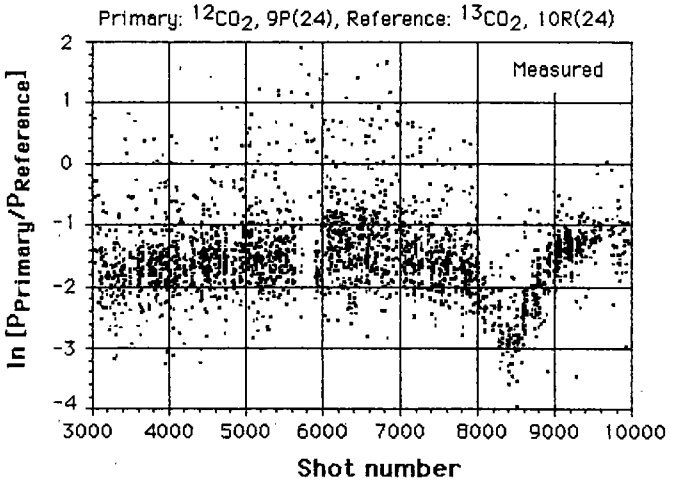

Fig. 7 Spectrum data measured with the RIS.

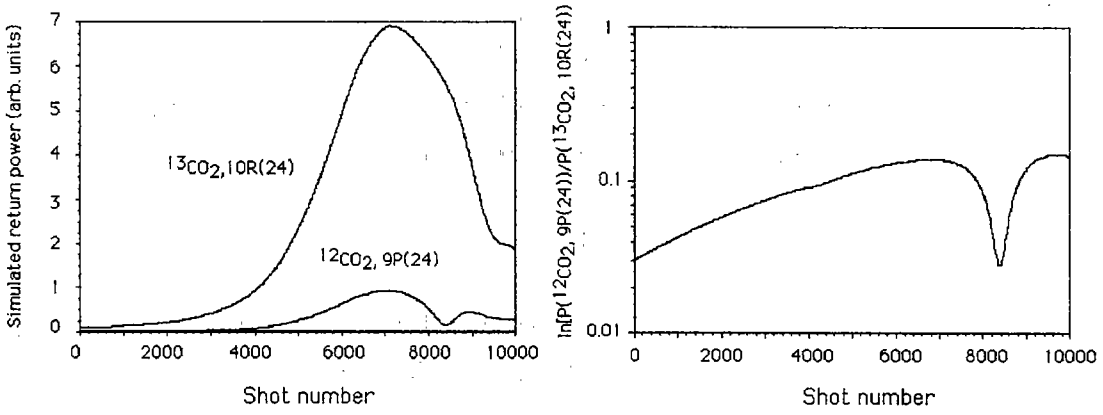

Fig. 8 Simulated signals for the RIS measurement.

We analyzed measurement error in the data taken with the RIS to evaluate the measurement method. There are various causes of noise in the received signals. They are detector noise, digitization noise of analog to digital converter, atmospheric turbulence, fluctuation of laser beam pattern, satellite tracking error, etc. Among them, the noise caused by atomospheric turbulence, beam fluctuation, and satellite tracking error is proportional to the recorded signal intensity. On the other hand, detector noise and digitization noise are independent of the signal intensity. To identify the dominant cause of the measurement error, we analyzed the dependence of the error on the signal intensity.

Figure 9 shows the square of the standard deviation of (P_{pri}/P_{ref}) as a function of the square of ($1/P_{ref}$). Both primary and reference lasers were tuned to 10P24 of $^{12}CO_2$. The standard deviation of (P_{pri}/P_{ref}) can be written as

$$<\Delta(P_1/P_2)^2>/(P_1/P_2)^2 = <\Delta P_1/P_1>^2 + <\Delta P_2/P_2>^2 - 2<\Delta P_1 \Delta P_2>/(P_1 P_2), \qquad (3)$$

where P_1, P_2 represent the averaged received power for primary and reference lasers, and ΔP_1, ΔP are their deviations. The third term in Eq(3) represents covariance. If the deviations in P_1 and P_2 are correlated, the third term cancels the first and the second terms in Eq(3). In the actual signals, there are correlated component and noncorrelated component.

Deviation of received power for each laser can be written as

$$<\Delta P>^2 = A + B\,P^2, \tag{4}$$

where the first term represents the noise independent of the signal intensity. The second term represents the noise proportional to the signal intensity. We may write the dependence of $<\Delta(P_1/P_2)^2>$ on the signal intensity in the same way as

$$<\Delta(P_1/P_2)^2>/(P_1/P_2)^2 = A'/P^2 + B', \tag{5}$$

where we assumed $P_1=P_2=P$. The slope of the plot in Fig.15, consequently, indicates the contribution of the noise independent of the received signal intensity, and the constant indicates the noise proportional to the signal intensity.

Figure 9 (a) shows a data taken with the RIS before improvement of the transmitter system. We calculated standard deviation for the data sets consisting of 10 successive pulsepairs. The constant term in Eq(5) is large in this case, and it can be concluded that the noise component proportional to the signal intensity is dominant. We found that the largest cause of the noise was the difference in the transmitted CO_2 beams from the two lasers, though both lasers had a TEM00 transverse mode. To improve the transmitted beam pattern, we added a spatial filter which consists of a pair of lenses, a pinhole, and apertures to the transmitter optics after combining the two beams. Figure 9(b) shows the result after the improvement of the transmitter. The noise proportional to signal intensity was reduced. We cannot compare the noise component independent of signal intensity in Fig. 9, because P in the figure is in a relative scale.

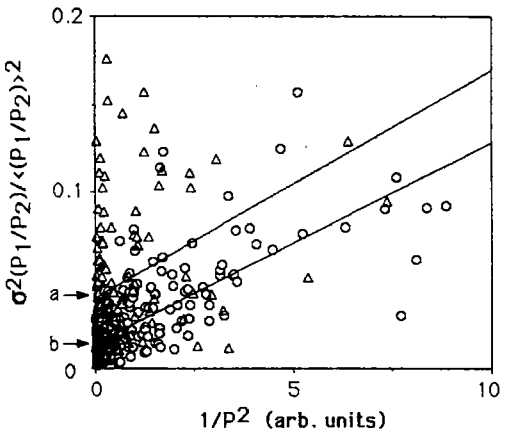

Fig. 9 The square of error in (P_{pri}/P_{ref}) as a function of the square of $(1/P_{ref})$.

We also studied the power spectrum of shot to shot variation of the received signal intensity and the ratio of signals for the two lasers. We used the Lomb method (Lomb 1976) to derive power

spectrum instead of regular fast Fourier transformation because data points were sometimes missing. Figure 10 shows the results. Upper panel shows the power spectrum of the signal intensity, and the lower panel shows that for the ratio of the signals. Trace (a) indicates the data taken before the improvement of the system. Trace (b) shows the data after the improvement using the spatial filter. Trace (c) shows the data after further improvement on the satellite tracking system. The noise component having a frequency around 0.6-0.8 Hz is the satellite tracking error. This noise component is seen also in the ratio of the signals in trace (a), but it is improved in trace (b). This shows that difference of the beam pattern of the two lasers was the cause of noise before using the spatial filter. After the improvement of the satellite tracking system, the noise component is small even in the power spectrum of signal intensity. In all cases in Fig. 10, noise with higher frequency component which may be caused by interference in a retroreflector array is not seen. This shows the feature of the RIS having a single element structure.

We obtained the signal-to-noise ratio of approximately 10 in the ratio of the received signal with the improved system. It correspond to the error of approximately 2 percent in the column contents of ozone.

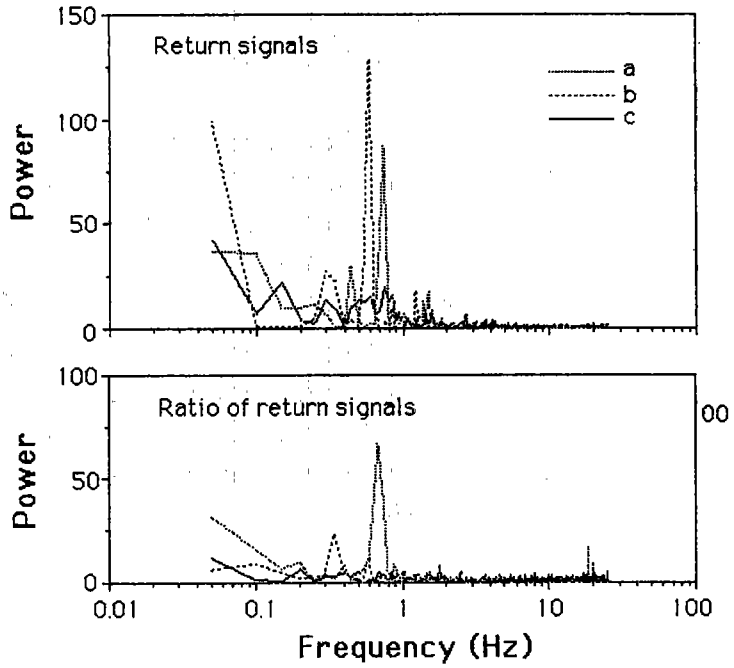

Fig. 10 Power spectrum of signal intensity (upper) and the ratio of the signals for the two lasers (lower).

5. Conclusion

We demonstrated the earth-satellite-earth laser long-path absorption method for measuring atmospheric trace species for the first time using the RIS. We measured absorption spectrum of atmospheric ozone using the Doppler shift method and obtained column contents. We validated the measurement with a simultaneous heterodyne spectrometer measurement. Because of the unexpected discontinuance of the ADEOS operation, we were not able to implement all experiments originally planned. However, we obtained useful data for evaluating the measurement technique. We are conducting feasibility study of the atmospheric monitoring system based on laser long-path absorption between the ground and a geosynchronous satellite (Sugimoto 1987, Sugimoto 1995c).

References

Fukunishi H, Okano S, Taguchi M and Ohnuma T 1990, "Laser heterodyne spectrometer using a liquid nitrogen cooled tunable diode laser for remote measurements of atmospheric O3 and N2O," *Appl. Opt.* **29** 2722-2728

Hinkley E D ed 1976 *Laser Monitoring of the Atmosphere* (Springer-Verlag) Chap. 6

Lomb N R 1976 *Astrophysics and Space Science* **39** 447-462

Minato A, Sugimoto N and Sasano Y 1992, "Optical Design of Cube-Corner Retroreflectors Having Curved Mirror Surfaces", *Appl. Opt*. **31** 6015-6020

Nordstrom R J, Berg L J,DeSimone A F and Sugimoto N 1993, "Time-Gated Gain Cell for Frequency-Stable, Single-Longitudinal-Mode Operation of a Transverse, Electric, Atmospheric CO_2 Laser," *Rev. Sci. Instrum.* **64** 1663-1664

Nordstrom R J, Berg L J, DeSimone A F and Sugimoto N 1994, "Single-Longitudinal-Mode Operation of a TEA CO2 Laser using a time gated gain cell," *Rev. Laser Eng.* **22** 132-139

Ozawa K, Sugimoto N, Koga N, Kubota Y, Saito Y, Nomura A , Minato A, Aoki T, Itabe T and Kunimori H 1997a, "Optical Characteristics of the Retroreflector in Space(RIS) on the ADEOS Satellite in Orbit," *Opt. Rev.***4** 450-452

Ozawa K, Koga N, Sugimoto N, Saito Y, Nomura A, Aoki T, Itabe T and Kunimori H 1997b, "Laser Transmitter/Receiver System for Earth-Satellite-Earth Long-Path Absorption Measurements of Atmospheric Trace Species Using the Retroreflector In Space," *Opt. Eng.* **36** (12) 3235-3241

Sugimoto N 1987, "Atmospheric environment monitoring system based on an earth-to-satelite Hadmard transform laser long-path absorption spectrometer: a proposal, " *Appl.Opt.* **26** 763-764

Sugimoto N, Minato A and Sasano Y 1991 *Conference on Lasers and Electro-Optics Technical Digest Series*, vol. **10** (Washington DC., 1991) p 450

Sugimoto N and Minato A 1994, "Method for measuring dihedral angles of a cube-corner retroreflector having curved mirror surfaces", *Opt. Eng.* **33** (4) 1187-1192

Sugimoto N, Minato A, Matsui I, Sasano Y, Itabe T, Aoki T, Takabe M, Hiromoto N and Kunimori H 1995a *SPIE* **2583** 217-227

Sugimoto N and Minato A 1995b, "Data Reduction Method for the Laser Long-Path Absorption Measurement of Atmospheric Trace Species Using the Retroreflector in Space, *IEICE Trans. Common.* **E78-B** 1585-1590

Sugimoto N, Minato A, Ozawa K, Saito Y, Nomura A 1995c, "Theoretical evaluation of earth-to-satellite laser long-path absorption measurement of atmospheric trace species in the infrared region," *Jpn. J. Appl. Phys.* **34** 2329-2334

Sugimoto N and Minoto A 1996, "Optical Characteristic of the Retroreflector in Space (RIS) for the ADEOS Satellite, *Opt. Rev.* **3**, 62-64